Article

Discovery Medicine 2024; 36(187): 1692–1702
https://doi.org/10.24976/Discov.Med.202436187.155

Hypoxia-Induced Ephrin-B2 Facilitates Proliferation and Induces Glycolytic Metabolism in Cutaneous Squamous Cell Carcinoma by Modulating PKM2/HIF-1α Axis

Xiaoqing Wang[1], Zheng Zhang[1], Guanglei Hu[2], Xiaobo Zhou[1,*]

[1]Department of Dermatology, Shanghai Ninth People's Hospital, Shanghai Jiao Tong University School of Medicine, 200011 Shanghai, China
[2]State Key Laboratory of Medical Neurobiology and MOE Frontiers Center for Brain Science, Institutes of Brain Science, Fudan University, 200032 Shanghai, China
*Correspondence: 19145711472@163.com (Xiaobo Zhou)
Published: 20 August 2024

Background: Cutaneous squamous cell carcinoma (cSCC) is a fatal disease characterized by metabolic dysregulation. The role of ephrin type-B receptor 2 (ephrin-B2), a crucial molecule in cancer cell biology, in regulating glycolysis and cell proliferation of cSCC is not well understood. This study aimed to investigate the biological pathways by which ephrin-B2 impacts the glycolysis and cell proliferation of cSCC.

Methods: Ephrin-B2 expression levels in cSCC were determined using quantitative reverse-transcription polymerase chain reaction (qRT-PCR) and Western blotting. *Ephrin-B2* expression in cSCC cells was manipulated using overexpression and knockdown approaches. A series of *in vitro* assays, such as cell counting kit-8 (CCK-8), Transwell assay, immunofluorescence assay, enzyme-linked immunosorbent assay (ELISA), qRT-PCR, and Western blotting, were employed to delineate the biological roles of ephrin-B2/pyruvate kinase muscle isoenzyme 2 (PKM2)/hypoxia-inducible factor 1 alpha (HIF-1α) in proliferation, migration, invasion, and glucose metabolism of cSCC.

Results: This study highlights an upregulation of *ephrin-B2* expression in cSCC. Knockdown of *ephrin-B2* significantly suppressed the proliferation, migration, invasion, and glucose metabolism of cSCC cells. Moreover, *ephrin-B2* expression was upregulated under hypoxic conditions. At the molecular level, *ephrin-B2* knockdown resulted in the downregulation of *PKM2* and *HIF-1α* expression. Additionally, the overexpression of *PKM2* or *HIF-1α* successfully rescued the diminished proliferation, migration, invasion and glucose metabolism induced by *ephrin-B2* knockdown in cSCC cells.

Conclusion: These findings suggest that ephrin-B2 suppression may hinder cSCC cell proliferation and glycolytic metabolism, potentially via the PKM2/HIF-1α axis modulation.

Keywords: ephrin-B2; cutaneous squamous cell carcinoma; PKM2; HIF-1α; glycolysis

Introduction

Cutaneous squamous cell carcinoma (cSCC) is a prevalent cancer characterized by uncontrolled cell proliferation and aberrant metabolic activities [1]. Emerging evidence suggests that alterations in cellular metabolism play a pivotal role in cancer progression, prompting an in-depth exploration of the molecular mechanisms governing these processes [2,3]. In the ever-evolving research landscape of tumor microenvironments, hypoxia—or reduced oxygen level—emerges as a crucial factor influencing cancer biology [4,5].

Hypoxia creates a selective pressure on cancer cells, prompting adaptive responses that facilitate survival and proliferation [6]. Within this hypoxic milieu, a myriad of molecular players orchestrate complex cellular processes [7]. Among them, ephrin type-B receptor 2 (ephrin-B2), a member of the ephrin family, has been implicated in diverse cellular functions and processes, including angiogenesis and vascular development [8]. A recent study has brought to light the involvement of ephrin-B2 in the progression of cancer, particularly its response to hypoxic conditions [9].

Hypoxia-inducible factor 1 alpha (HIF-1α) serves as a master regulator, driving cellular responses to reduced oxygen levels [10]. HIF-1α orchestrates adaptive changes, including alterations in glucose metabolism, to meet the energy demands of rapidly proliferating cancer cells [11]. Concurrently, pyruvate kinase muscle isoenzyme 2 (PKM2), a pivotal enzyme in glycolysis, is a central player in cancer metabolism [12], regulating energy production and biosynthetic pathways crucial for cancer cell survival [13].

Substantial progress has been achieved in understanding the disparate roles of ephrin-B2, PKM2, and HIF-1α in cancer biology and metabolism, but the interplay be-

tween these players in cSCC progression has yet to be comprehensively deciphered. This knowledge gap underscores the need for detailed investigations to unravel the intricate crosstalk among these molecular players and delineate the PKM2/HIF-1α axis and their collective impact on cell proliferation and carbohydrate metabolism in cSCC.

The objective of this study is to investigate the complex molecular mechanisms involving hypoxia-induced ephrin-B2 and the PKM2/HIF-1α axis, and to clarify their collective impact on cSCC. A deeper understanding of these complex molecular networks can facilitate the development of potential therapeutic targets and strategies tailored for cSCC under hypoxic conditions.

Materials and Methods

Cell Cultures

Normal human epidermal keratinocytes (NHEK) cells (QS-H226) and human cutaneous squamous cell carcinoma cell lines A431 (QS-H162) and SCC-13 cells (QS-H176) were purchased from Keycell Inc (Wuhan, China). These cells were cultured in Dulbecco's Modified Eagle Medium (DMEM) supplemented with 10% fetal bovine serum and 1% penicillin-streptomycin. The cells were cultivated in an incubator set at 37 °C and 5% CO_2. Regular medium replacement was performed to ensure the continual provision of fresh nutrients, so as to support the robust growth of cancer cells. Subculturing was conducted when the cancer cells reached an 80% fusion rate to prevent over-confluence. The cell lines used in this study have all undergone Short Tandem Repeat (STR) profiling and tested negative for mycoplasma contamination.

Cell Transfection

The cells were cultured until reaching 70–80% confluence. Sh-RNA and pCMV plasmids were custom-ordered from Sangon Biotech (Shanghai, China). The shRNA and pCMV plasmids utilized in this study and their corresponding sequences are as follows: Sh-NC (sense: 5′-TTCTCCGAACGTGTCACGT-3′, antisense: 5′-ACGTGACACGTTCGGAGAA-3′), Sh-*ephrin-B2* (sense: 5′-GCTGCTGAAGAAGAAATAT-3′, antisense: 5′-ATATTTCTTCTTCAGCAGC-3′), pCMV-blank plasmid (sense: 5′-GCTAGCATCTGAGGACTAG-3′, antisense: 5′-CTAGTCTCAGATGCTAGC-3′), pCMV-*PKM2* plasmid (sense: 5′-ATGGAAGCCGTGATGCTG-3′, antisense: 5′-CTAAGCCACAGCTTCTGCTC-3′), pCMV-*HIF-1*α plasmid (sense: 5′-ATGTCTGCCCTTCACCTG-3′, antisense: 5′-TTAGTTGGGACTTGAGGTT-3′). To conduct shRNA or pCMV-plasmid transfection, the aforementioned Sh-RNA or pCMV-plasmid was separately used to treat the cultured cells in the presence of Lipofectamine 3000 transfection reagent (L3000001, Thermo Fisher Scientific, Shanghai, China). The transfection complex was then diluted in serum-free Opti-MEM medium, and the mixture was evenly distributed by gently rocking the culture dish. Subsequently, the Opti-MEM medium was replaced with complete medium containing 10% fetal bovine serum, and the cells were returned to incubation under the conditions of 37 °C and 5% CO_2 for 48 hours. Transfection efficiency was evaluated through quantitative reverse-transcription polymerase chain reaction (qRT-PCR) or Western blotting analysis.

Table 1. Sequences of primers used in qRT-PCR.

Gene	Primer sequences (5′–3′)
Ephrin-B2 (F)	ATGGCCTGTCTGTGCTGGT
Ephrin-B2 (R)	TCAGCAGCGGAGCAGGA
GLUT1 (F)	ATGGCGGTGTGGGTCGTGG
GLUT1 (R)	TCCAGGCTGCAGTGGTGGTG
LDHA (F)	ATGGAAACTCTGGAGATG
LDHA (R)	TTAGGTTGATGGGTAGGA
β-actin (F)	ACACTGTGCCCATCTACG
β-actin (R)	TGTCACGCACGATTTCC

qRT-PCR, quantitative reverse-transcription polymerase chain reaction; *ephrin-B2*, ephrin type-B receptor 2; *GLUT1*, Glucose Transporter Type 1; *LDHA*, Lactate Dehydrogenase A.

RNA Extraction and Quantitative Reverse-Transcription Polymerase Chain Reaction

Total RNA was extracted from the cells using the TRIzol method (DP424, Tiangen Biotech (Beijing) Co., Ltd., Beijing, China), followed by reverse transcription of RNA into corresponding cDNA using reverse transcriptase (KR116, Tiangen, Beijing, China). Target gene cDNA amplification was performed using specific primers and DNA polymerase. Fluorescent probes or dyes (FP205, Tiangen Biotech (Beijing) Co., Ltd., Beijing, China) were added to the reaction mixture used in the PCR experiment, with the fluorescence intensity directly correlating to target gene amplification. The PCR cycles were monitored in real-time, and the fluorescence signal intensity was measured using fluorescent quantitative PCR instrument (LightCycler96, Roche, Basel, Switzerland). 95 °C, denaturation for 30 seconds; 60 °C, annealing for 20 seconds; 72 °C, extension for 60 seconds, 30 cycles. Relative expression levels of the target genes across different samples were calculated by comparing their fluorescence signals to those of a control group (e.g., *β-actin*). The $\Delta\Delta$Ct method or other mathematical models were employed in data analysis and normalization to determine the target gene expression levels under varied conditions. Specific primers and their sequences used in this chapter are provided in Table 1.

Western Blotting

Total proteins were extracted from cells by protein extraction kit (P0027, Beyotime, Shanghai, China), followed by determination of protein concentration using a BCA assay kit (E112-01, Vazyme, Nanjing, China). The extracted

protein samples were then separated via sodium dodecyl sulfate-polyacrylamide gel electrophoresis (SDS-PAGE). Subsequently, the separated proteins were transferred from the gel onto a solid membrane (PVDF). Blocking buffer was applied to the membrane to prevent nonspecific binding. The membrane was then incubated with antibodies, namely ephrin-B2 (1:1000; cat no, ab131536; Abcam, Cambridge, UK), PKM2 (1:1000; cat no, ab85555; Abcam, Cambridge, UK), HIF-1α (1:1000; cat no, ab308433; Abcam, Cambridge, UK), and Glyceraldehyde 3-phosphate dehydrogenase (GAPDH) (1:1000; cat no, ab8245; Abcam, Cambridge, UK), for 2 h at 37 °C. After washing to reduce background signals, the membrane was incubated with secondary antibodies (Rabbit Anti-Mouse IgG H&L (HRP)), from a different species than the primary antibodies (1:2000; cat no, ZB-2301; ZSGB-BIO, Beijing, China) for 2 h at 37 °C. Following another wash to minimize background signals, chemiluminescent or staining techniques were employed to detect proteins labeled with secondary antibodies to generate visible signals. Quantitative analysis of the target protein's signal intensity in the samples was conducted by comparison to standard curves. Data analysis and image processing were performed using ImageJ software (version 1.5f, National Institutes of Health, Bethesda, MD, USA).

Cell Counting Kit-8 (CCK-8) Assay

Following transfection with vectors, the A431 and SCC-13 cells were suspended in culture medium and seeded into culture dishes until achieving an optimal confluence. After 24 hours of continuous cultivation, CCK-8 reagent was added to each culture dish, covering the entire cell layer. The cells were then incubated for an additional 2 hours to facilitate the reaction between the CCK-8 reagent (CA1210, Solarbio, Beijing, China) and the cells. Following this, the absorbance was assessed at a wavelength of 450 nm employing either a microplate reader or a multifunctional enzyme-linked immunosorbent assay (ELISA) reader (Cmax plus, Molecular Devices Corporation, Silicon Valley, CA, USA).

Immunofluorescence Assay

Briefly, cSCC cells were suspended in culture medium and cultivated for 12 hours. Subsequent steps included cell fixation and permeabilization, followed by staining using the EdU Fluorometric Assay Kit (C0078S, Beyotime, Shanghai, China), which employs click chemistry reaction to conjugate EdU with a fluorescent dye. Additionally, co-labeling was performed using a nuclear staining dye (DAPI) (C1002, Beyotime, Shanghai, China). Finally, fluorescently labeled cells were observed and imaged with a fluorescence microscope (Axio Observer, Zeiss, Jena, Germany). Quantitative analysis was conducted to calculate the percentage of EdU-positive cells, providing an assessment of DNA synthesis activity.

Transwell Assay

Evaluation of Cell Migration

Transwell inserts were first installed onto a Transwell plate, which were optionally pre-treated with extracellular matrix proteins like Matrigel. Cell suspension was added to the upper chamber of the Transwell inserts. In the lower chamber, culture medium was added, and the Transwell plate was then placed in a CO_2 incubator for 2 h at 37 °C. After incubation, the Transwell inserts were subjected to washing, prior to cell fixation. The cells in the upper chamber were stained with agents such as crystal violet. Lastly, the cells in the upper chamber were observed under a microscope (CX53, Olympus, Tokyo, Japan). The number of migrated cells were determined from the images captured with the microscope (CX53, Olympus, Tokyo, Japan).

Evaluation of Cell Invasion

To study cell invasion, the experiment started with pre-treating the Transwell inserts with Matrigel to simulate the basement membrane. Cell suspension was then added to the upper chamber of the Transwell inserts, while culture medium was added to the lower chamber. Subsequently, the Transwell plate was incubated in a CO_2 incubator for 2 h at 37 °C. Afterward, the Transwell inserts were subjected to washing, prior to cell fixation. Crystal violet was utilized to stain invasive cells that had penetrated the matrix. Finally, the cells in the lower chamber were observed under a microscope (CX53, Olympus, Tokyo, Japan). The number of invading cells was counted from the images captured with the microscope (CX53, Olympus, Tokyo, Japan).

Glucose Uptake Assay

Prepare cells containing glucose. A series of standard glucose solutions with known concentrations were prepared to generate a standard curve for quantification. The assay reagents provided in the glucose assay kit (BC2505, Solarbio, Beijing, China) were prepared according to the manufacturer's instructions. Prepared samples, standard solutions, and appropriate controls were separately added into the wells of a microplate or test tubes. The assay reagents were added to each well or tube containing samples, standard solutions, or controls. The reaction mixture was incubated at 37 °C for 2 h to facilitate enzyme reactions. After incubation, the absorbance of each well was measured at a wavelength of 505 nm using a microplate reader (Cmax plus, Molecular Devices Corporation, Silicon Valley, CA, USA). The absorbance values of the standard solutions were utilized to plot a standard curve, through which the concentration of glucose in the samples was determined. Relative glucose concentration was calculated using the formula in the following:

$$\text{Relative glucose concentration} = \text{Experimental group/Control group} \times 100\%$$

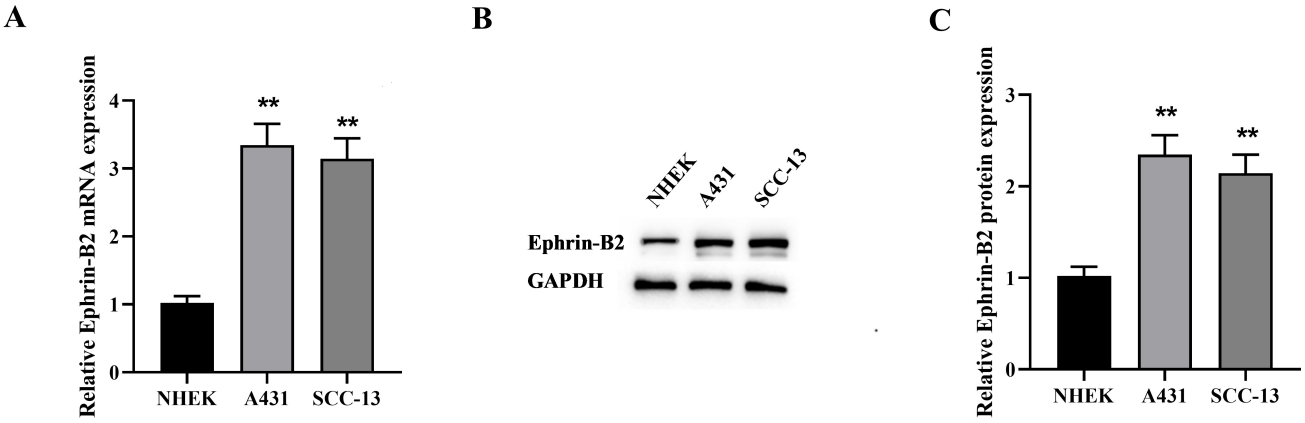

Fig. 1. Upregulated ephrin-B2 expression in cutaneous squamous cell carcinoma (cSCC). (A) mRNA expression levels of *ephrin-B2* in normal human epidermal keratinocytes (NHEK) cells, A431 cells, and SCC-13 cells, as detected by qRT-PCR. (B,C) Protein expression levels of ephrin-B2 in NHEK cells, A431 cells, and SCC-13 cells, as detected by Western blotting. n = 6; $^{**}p < 0.01$. GAPDH, Glyceraldehyde 3-phosphate dehydrogenase.

Lactic Acid Production Assay

Lactate-containing cells and a series of standard lactate solutions with known concentrations were prepared to establish a standard curve for quantitative analysis. The assay reagents provided in the lactate assay kit (BC2235, Solaibao Technology Co., Ltd., Beijing, China) were prepared in adherence with the manufacturer's instructions. The prepared samples, standard solutions, and appropriate controls were separately added into the wells of a microplate. Then, the lactate assay reagents were added to each well containing samples, standard solutions, or controls. The reaction mixture was incubated at 37 °C for 2 h to facilitate enzyme reactions. After incubation, the absorbance of each well was determined at a wavelength of 450 nm using a microplate reader (Cmax plus, Molecular Devices Corporation, Silicon Valley, CA, USA). The absorbance values obtained from the standard solutions were utilized to plot the standard curve, through which the lactate concentration in the samples was determined. Relative lactic acid concentration was calculated using the following in the following:

$$\text{Relative lactic acid concentration} = \text{Experimental group/Control group} \times 100\%$$

Adenosine Triphosphate (ATP)/Adenosine Diphosphate (ADP) Assay

Total cellular extracts containing ATP and ADP were obtained by lysing the cells using a cell lysis buffer. The content of ATP and ADP in the samples was determined using an ATP/ADP Ratio Assay Kit (MAK135-1KT, Merck, Darmstadt, Germany). The ATP and ADP levels in the samples were measured using a microplate reader (Cmax plus, Molecular Devices Corporation, Silicon Valley, CA, USA). Reaction conversion rate was adjusted, if ADP converted to ATP during measurement. The ATP/ADP ratio was calculated based on the measured ATP and ADP levels. The changes in the ATP/ADP ratio of the samples were analyzed based on the experimental data obtained.

Statistical Analyses

The results are presented as mean ± standard deviation. Statistical significance was considered at $p<0.05$. Statistical analyses were conducted using GraphPad Prime software 8.0 (GraphPad Prime Inc, San Diego, CA, USA, available at https://www.graphpad-prism.cn/). *t*-tests and ANOVA coupled with Tukey's post hoc analysis were performed to statistically identify significant differences and trends.

Results

Ephrin-B2 Expression is Upregulated in cSCC

To elucidate the expression pattern of ephrin-B2 in both normal and neoplastic cells, we quantified ephrin-B2 levels in normal human epidermal keratinocytes (NHEK cells) compared to human cutaneous squamous cell carcinoma cells (A431 and SCC-13 cells). Results of qRT-PCR and Western blotting indicated that the mRNA and protein expression of *ephrin-B2* in A431 cells and SCC-13 cells was significantly higher than in NHEK cells ($p < 0.01$) (Fig. 1A–C).

Ephrin-B2 Knockdown Inhibits Proliferation, Migration, and Invasion of cSCC

To elucidate the functional role of ephrin-B2 in cellular behaviors, we transfected A431 and SCC-13 cells with Sh-*ephrin-B2*. After 48 hours of cell transfection, proliferation, migration, and invasion of cSCC were assessed. The results demonstrated that Sh-*ephrin-B2* significantly downregulated the protein expression levels of *ephrin-B2*

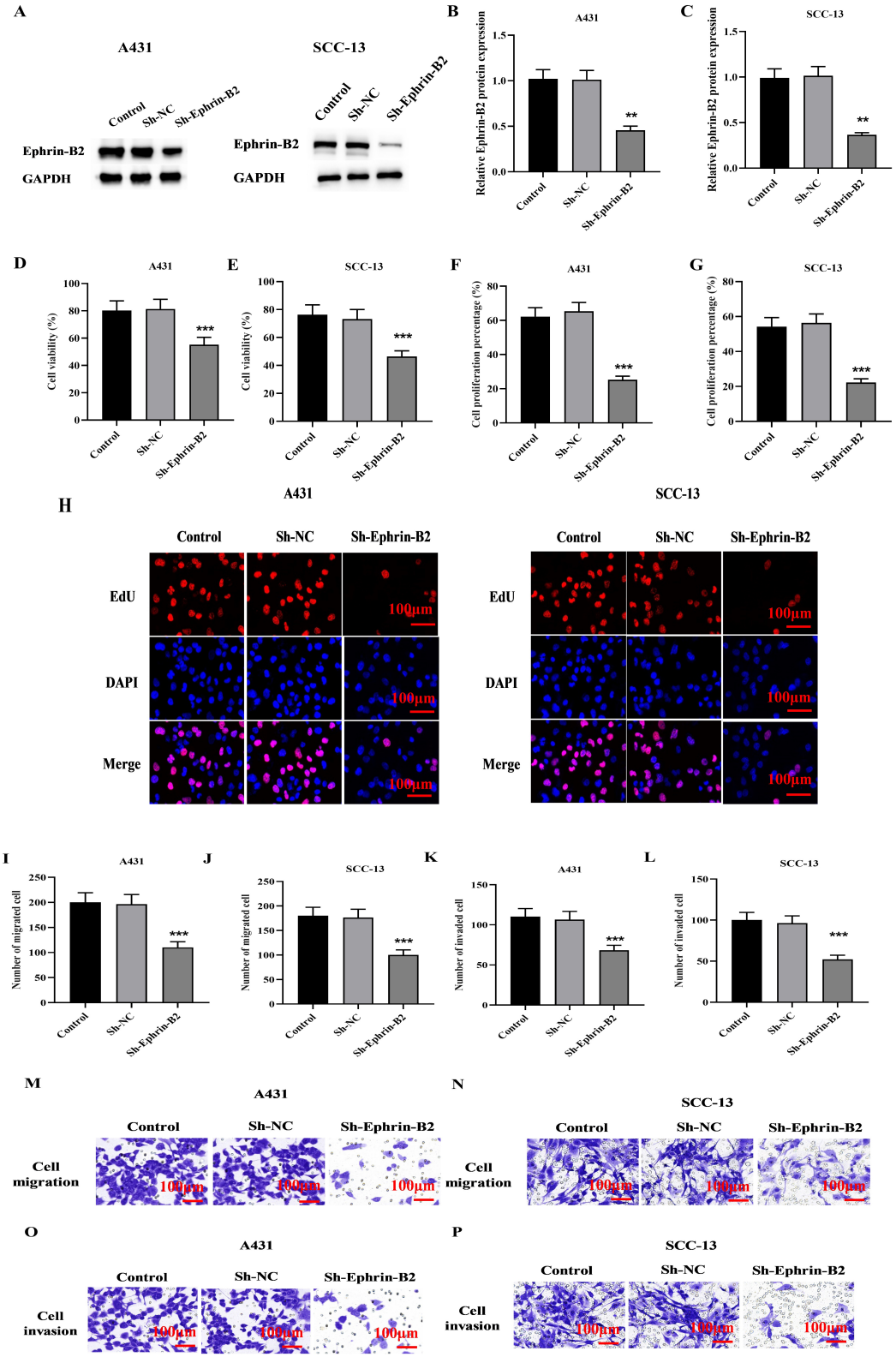

Fig. 2. The *ephrin-B2* knockdown inhibits proliferation, migration, and invasion of cSCC. (A–C) Determination of the gene knockdown effect of Sh-*ephrin-B2* in A431 and SCC-13 cells. (D,E) Determination of the inhibitory effect of Sh-*ephrin-B2* on the viability of A431 and SCC-13 cells through cell counting kit-8 (CCK-8) assay. (F–H) Analysis of the suppressive effect of Sh-*ephrin-B2* on the proliferation capacity of A431 and SCC-13 cells through EdU immunofluorescence. (I–P) Analysis of the impact of Sh-*ephrin-B2* on the migration and invasion capabilities of A431 and SCC-13 cells through Transwell assay. n = 6; $^{**}p < 0.01$, $^{***}p < 0.001$. NC, Negative control.

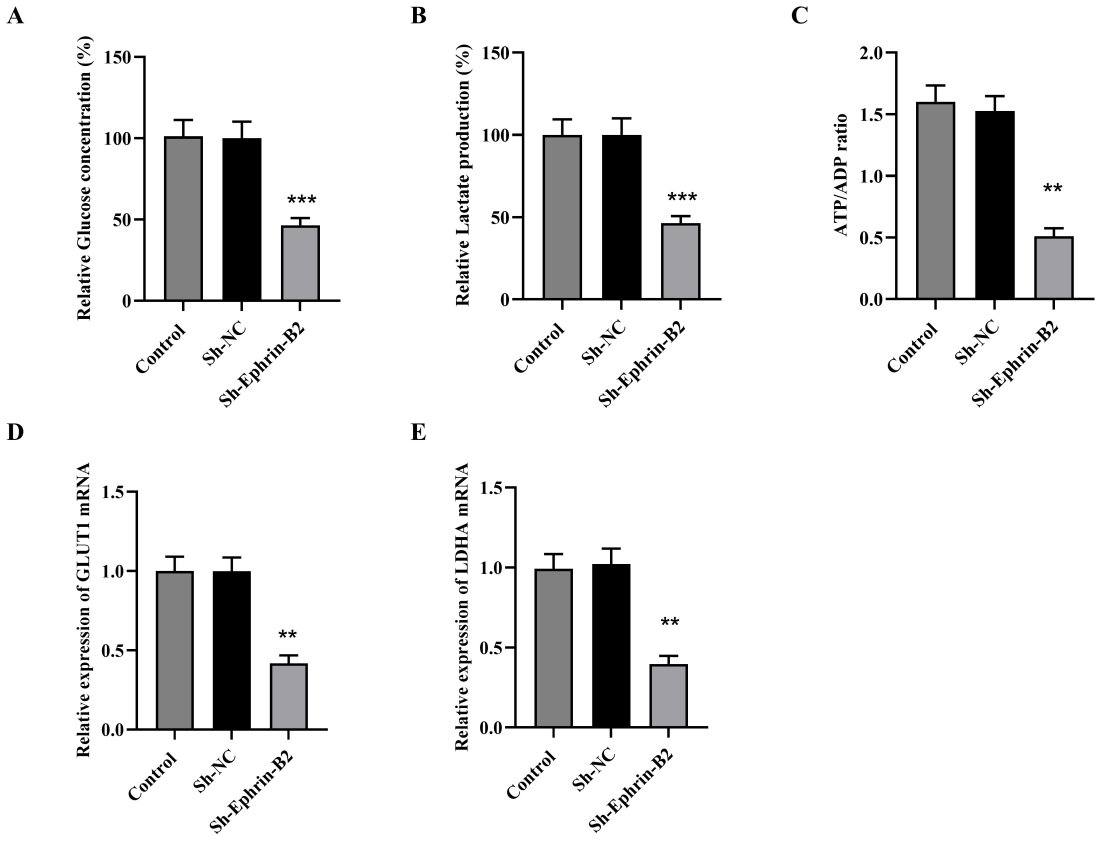

Fig. 3. Downregulation of *ephrin-B2* inhibits the glycolytic metabolism of cSCC cells. (A) Quantification of glucose levels in cSCC cells. (B) Assessment of lactate production in cSCC cells. (C) Determination of ATP/ADP ratio in cSCC cells. (D,E) mRNA expression of *GLUT1* and *LDHA* in cSCC cells. n = 6; $^{**}p < 0.01$, $^{***}p < 0.001$. ATP, Adenosine Triphosphate; ADP, Adenosine Diphosphate.

($p < 0.01$) (Fig. 2A–C). To investigate the biological role of ephrin-B2 in the progression of cSCC, we measured cancer cell proliferation using CCK-8 kit and EdU staining. These experimental results similarly showed that the knockdown of ephrin-B2 in A431 and SCC-13 cells significantly reduced cell viability and proliferation capacity ($p < 0.001$) (Fig. 2D–H). On the other hand, Transwell experiments were conducted to measure the migration and invasion capabilities of ephrin-B2 in cSCC cells. Compared to the negative control, the migration and invasion abilities of A431 and SCC-13 cells became suppressed following the downregulation of ephrin-B2 ($p < 0.001$) (Fig. 2I–P).

Downregulation of Ephrin-B2 Inhibits the Glycolytic Metabolism of cSCC Cells

Our next exploration primarily focused on glycolytic metabolism indicators. It is noteworthy that, following *ephrin-B2* knockdown, a significant reduction in glucose uptake, lactate production, ATP/ADP ratio, as well as mRNA levels of Glucose Transporter Type 1 (*GLUT1)* and Lactate Dehydrogenase A (*LDHA*) was observed in A431 cells ($p < 0.01$ and $p < 0.001$) (Fig. 3A–E). These findings underscore the critical role of ephrin-B2 in regulating the metabolic pathways that are essential for the proliferation and survival of cSCC cells.

Ephrin-B2 Regulates the Glycolytic Metabolism of cSCC Cells through the PKM2/HIF-1α Axis

Next, we explored the factors that upregulate ephrin-B2 expression in cSCC. Compared to normoxic conditions, hypoxic conditions or treatment with the hypoxia-inducing agent $CoCl_2$ for 24 hours significantly augmented the expression of *ephrin-B2* in A431 cells ($p < 0.05$ and $p < 0.01$) (Fig. 4A). Subsequently, we observed that the knockdown of *ephrin-B2* significantly reduced the protein levels of HIF-1α and PKM2 in A431 cells ($p < 0.01$) (Fig. 4B–D). To further validate the biological roles of PKM2 and HIF-1α in ephrin-B2, rescue experiments were conducted. *PKM2* overexpression plasmid or *HIF-1α* overexpression plasmid was transfected into *ephrin-B2*-knockdown A431 cells. The results showed that the glucose uptake, lactate production, ATP/ADP ratio, and mRNA levels of *GLUT1* and *LDHA* were significantly increased in the Sh-*ephrin-B2* + OE-*PKM2* and Sh-*ephrin-B2* + OE-*HIF-1α* treatment groups, as compared to the Sh-*ephrin-B2* + OE-NC (Negative control) group ($p < 0.01$, and $p < 0.001$) (Fig. 4E–I).

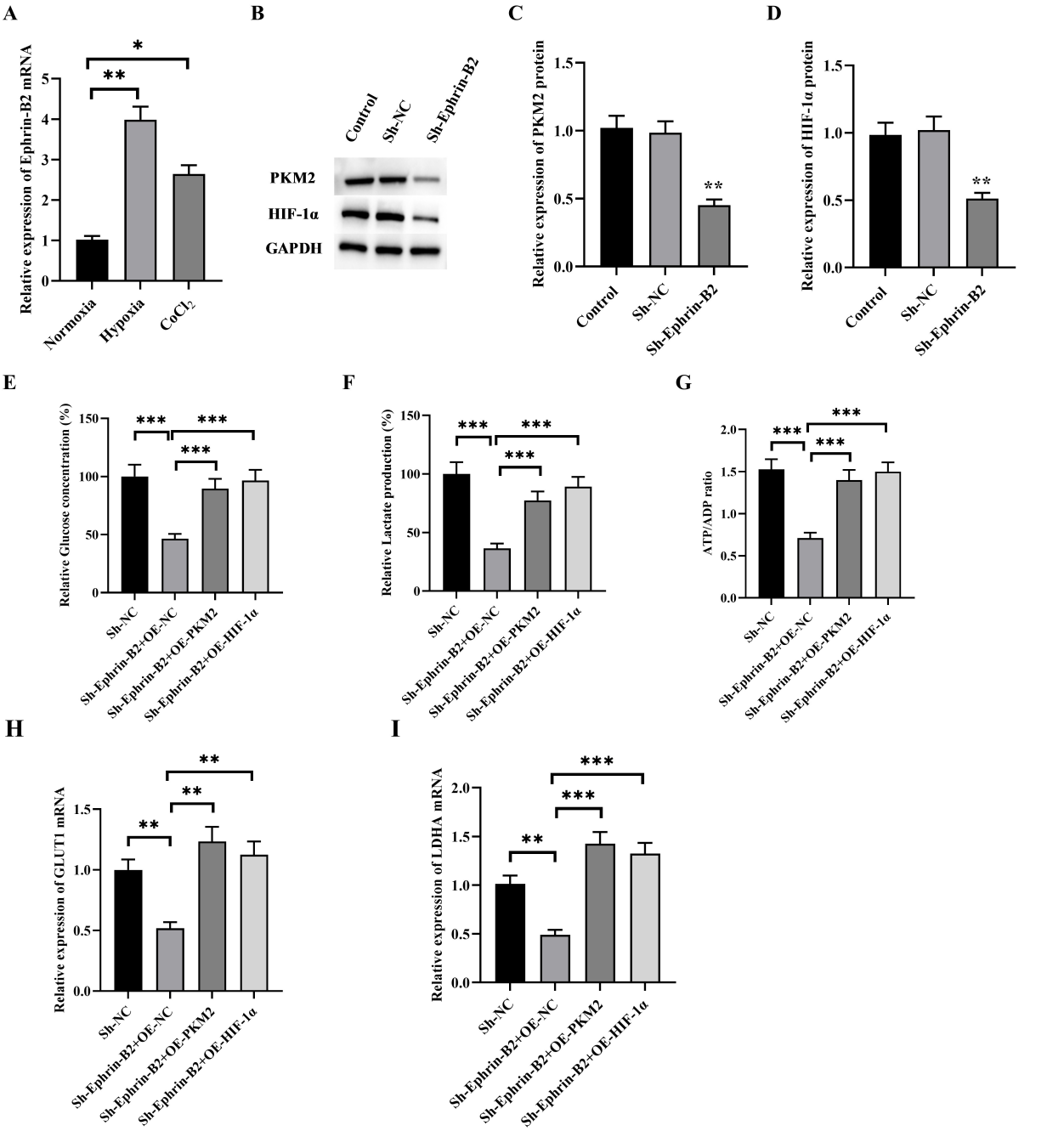

Fig. 4. Hypoxia-induced *ephrin-B2* modulates the glycolytic metabolism of cSCC cells via the pyruvate kinase muscle isoenzyme 2 (PKM2)/hypoxia-inducible factor 1 alpha (HIF-1α) axis. (A) *Ephrin-B2* mRNA expression levels in A431 cells following 24-hour cultivation under normoxia, hypoxia (1% O_2), or treatment with $CoCl_2$ (100 µM). (B–D) Reduced protein expression levels of PKM2 and HIF-1α in A431 cells following *ephrin-B2* knockdown. (E) Glucose uptake in *ephrin-B2*-knockdown A431 cells transfected with pCMV-PKM2 or pCMV-HIF-1α under hypoxic conditions. (F) Lactate production in cSCC cells. (G) ATP/ADP ratio in cSCC cells. (H,I) mRNA levels of *GLUT1* and *LDHA* in cSCC cells. n = 6; *$p < 0.05$, **$p < 0.01$, ***$p < 0.001$.

Hypoxia-Induced Ephrin-B2 Regulates the Proliferation, Migration, and Invasion of cSCC Cells through the PKM2/HIF-1α Axis

Subsequently, we further validated whether *ephrin-B2* regulates the cellular behaviors of cSCC through the PKM2/HIF-1α axis under hypoxic conditions. CCK-8 and EdU fluorescence analysis experiment results indicated that the activity and proliferation capacity of A431 cells were significantly augmented in the Sh-*ephrin-B2* + OE-*PKM2* and Sh-*ephrin-B2* + OE-*HIF-1α* treatment groups in hypoxic conditions, as compared to the Sh-*ephrin-B2* + OE-NC group ($p < 0.001$) (Fig. 5A,B,E). Additionally, Transwell experiment results demonstrated that the migration and invasion capabilities of A431 cells in the Sh-*ephrin-*

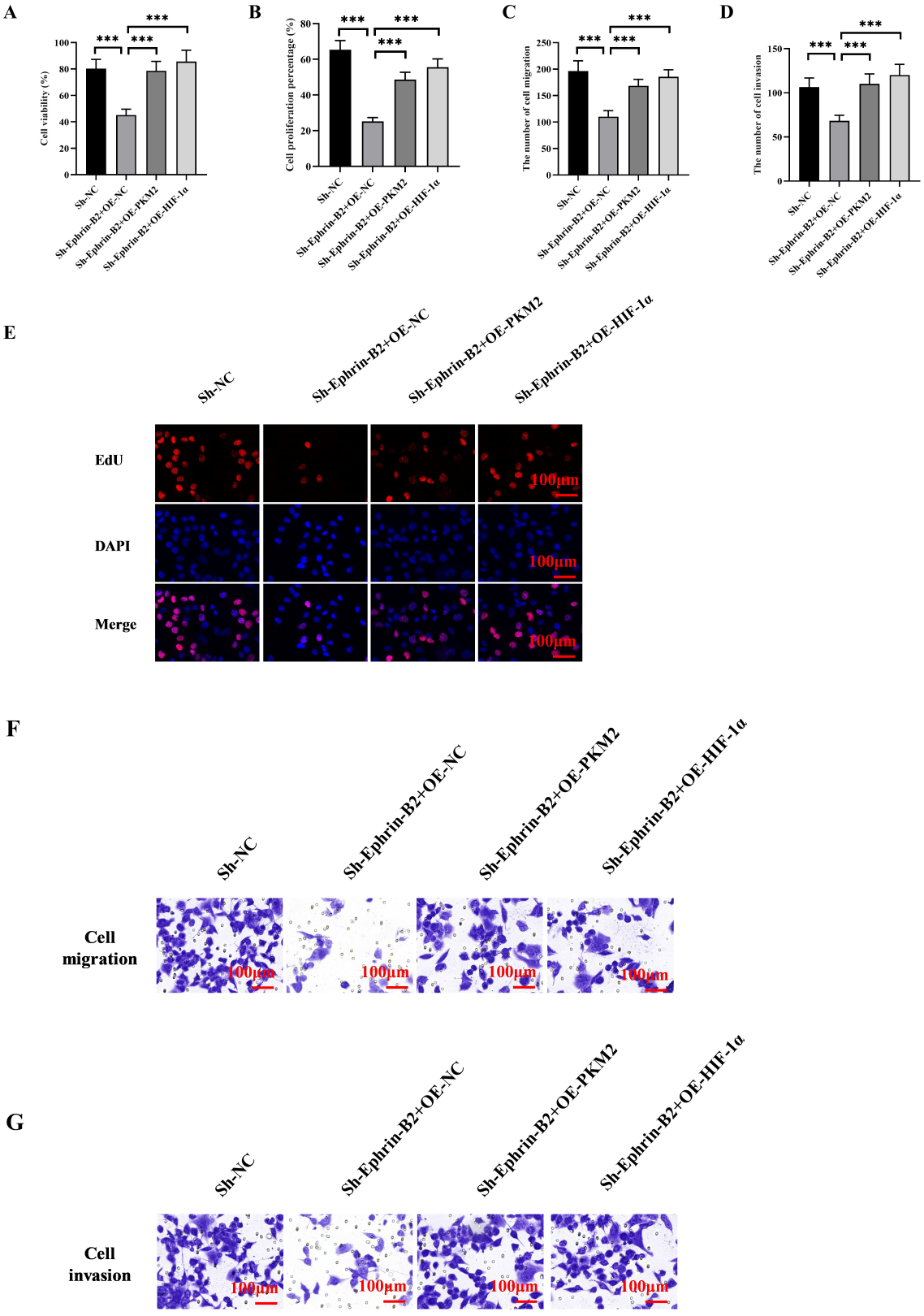

Fig. 5. Hypoxia-induced *ephrin-B2* modulates the proliferation, migration, and invasion of cSCC cells via the *PKM2*/*HIF-1*α axis. Under hypoxic conditions, pCMV-*PKM2* or pCMV-*HIF-1*α was transfected into A431 cells in which *ephrin-B2* expression had been downregulated. (A) Cell viability of A431 cells. (B,E) Quantitative presentation of A431 cell proliferation capacity (B) based on the EdU immunofluorescence results (E). (C,D,F,G) Quantitative presentation of migration (C) and invasion capabilities (D) of A431 cells based on the Transwell assay results (F,G). n = 6; ***$p < 0.001$.

B2 + OE-*PKM2* and Sh-*ephrin-B2* + OE-HIF-1α treatment groups were significantly higher than those in the Sh-*ephrin-B2* + OE-NC group ($p < 0.001$) (Fig. 5C,D,F,G).

Discussion

Numerous dysregulated genes have been extensively studied in the context of human cSCC, among which ephrin-B2 has garnered widespread attention as it provides a novel direction for exploring the molecular pathways involved in cSCC progression [14]. The overexpression of ephrin-B2 is associated with tumor vascularization, which is crucial for the growth and metastasis of tumors [15]. Therefore, exploring the biological functions of ephrin-B2 may enhance our understanding of the regulatory mechanisms in the biological processes of cSCC. In the present study, we found that ephrin-B2 has a high-expression pattern in cSCC. Consistent with our findings, ephrin-B2 is also reportedly overexpressed in head and neck squamous cell carcinoma, showing a close association with proteins linked to poor prognosis [16].

Due to the sensitivity of most cancer cells to hypoxic conditions, we sought to understand how cancer cells adapt to survive in a cellular stress microenvironment. Previous studies indicate that metabolic plasticity is crucial for cancer cells to survive in challenging nutrient-deprived environments [17]. Our current research suggests that ephrin-B2 is a stress-responsive molecule that promotes metabolic plasticity under stressful conditions. Additionally, the expression of ephrin-B2 is significantly elevated under hypoxic conditions. This finding aligns with a study conducted by Shang *et al.* [18]. Mechanistic analysis indicates that ephrin-B2 can influence the glycolysis of cSCC by modulating HIF-1α. A recent study has confirmed the pivotal role of HIF-1α in the glycolytic metabolism process [19]. For instance, LincRNA-p21 has been identified as a hypoxia-responsive long non-coding RNA (lncRNA), which is known to regulate the stability of HIF-1α protein. This reciprocal interaction establishes a positive feedback loop that enhances glycolysis in hypoxic conditions [20]. Wang *et al.* [21] found that HIF-1α can indirectly upregulate PKM2 by activating the Aly/REF export factor (ALYREF), thereby influencing the glycolysis of bladder cancer. Therefore, we hypothesize that ephrin-B2 is a potential key molecule coordinating glycolytic metabolism under hypoxic conditions.

Increasing evidence suggests that ephrin-B2 can interact with specific proteins to participate in overall cellular behaviors [22,23]. PKM2 is a specific isozyme that plays a crucial role in the glycolytic pathway. The main role of pyruvate kinase is to catalyze the conversion of phosphoenolpyruvate to pyruvate. Thus, regulating the activity of PKM2 in the glycolytic pathway is essential for meeting the energy demands of rapidly proliferating cancer cells [24,25]. The abnormal expression and localization of PKM2 have been confirmed in various human cancers [26,27]. Recent studies have indicated that cell signaling, angiogenesis, and tissue development are closely associated with glycolysis and cancer cell metabolism [28,29]. Given that ephrin-B2 is involved in various cellular processes, including axon guidance, angiogenesis, and vascular development, and that PKM2 plays a crucial role in cancer cell metabolism, we hypothesize that an interplay between ephrin-B2 and PKM2 influencing the occurrence and progression of cSCC might exist. Our findings in this study confirm the aforementioned hypothesis, evidenced by the alterations to the glycolytic process in cSCC, which resulted from the downregulation of PKM2 expression mediated by ephrin-B2 knockdown. The present study also confirmed that PKM2 functionally contributes to the cSCC progression driven by ephrin-B2. Another study proposed that LINC01554 inhibits the reprogramming of glucose metabolism by downregulating the expression of PKM2 in hepatocellular carcinoma [30].

In an oxygen-deprived microenvironment, HIF-1α is a master regulatory factor crucial for the survival of tumors, forming intricate link with PKM2 [31]. Hua *et al.* [32] found that lncRNA-AC020978 directly interacts with PKM2, thereby enhancing PKM2 protein stability, promoteing the nuclear translocation of PKM2, and regulating the PKM2-enhanced transcriptional activity of HIF-1α. According to a study by Wang *et al.* [33], JMJD5 is involved in regulating the nuclear translocation of PKM2 and reprogramming HIF-1α-mediated glucose metabolism. Our data revealed that ephrin-B2 may participate in the interaction between PKM2 and HIF-1α.

Hypoxia-induced upregulation of ephrin-B2 in cSCC, coupled with the abnormal activation of the PKM2/HIF-1α glycolytic cascade, may represent a metabolic adaptation of cancer cells, enabling their survival under hypoxic stress. In future studies, further efforts should be directed toward exploring how ephrin-B2 coordinates the rewiring of the glycolytic pathway in cSCC cells.

Conclusion

In conclusion, the inhibition of ephrin-B2 may hinder the proliferation and influence the glycolytic metabolism of cSCC cells, possibly through the modulation of PKM2/HIF-1α axis.

Availability of Data and Materials

Data to support the findings of this study are available on reasonable request from the corresponding author.

Author Contributions

XQW: conceptualization, methodology, formal analysis, writing - original draft; ZZ: data curation, writing - original draft, software, validation, writing - review & edit-

ing; GLH: conceptualization, software, investigation, writing - original draft; XBZ: visualization, acquisition of data, analysis of data, interpretation of data, resources, supervision, writing - review & editing. All authors contributed significantly to editorial changes of important content. All authors read and approved the final manuscript. All authors have participated sufficiently in the work and agreed to be accountable for all aspects of the work.

Ethics Approval and Consent to Participate

Not applicable.

Acknowledgment

Not applicable.

Funding

This research was funded by Fundamental research program funding of Ninth People's hospital affiliated to Shanghai Jiao Tong university School of Medicine (Grant No. JYZZ176).

Conflict of Interest

The authors declare no conflict of interest.

References

[1] Winge MCG, Kellman LN, Guo K, Tang JY, Swetter SM, Aasi SZ, *et al*. Advances in cutaneous squamous cell carcinoma. Nature Reviews. Cancer. 2023; 23: 430–449.

[2] Kitamura S, Maeda T, Yanagi T. Vandetanib inhibits cell growth in EGFR-expressing cutaneous squamous cell carcinoma. Biochemical and Biophysical Research Communications. 2020; 531: 396–401.

[3] Xue C, Yang Z, Yang B, Xiong H, Ye W. LINC00460 Promotes Cutaneous Squamous Cell Carcinoma Progression Through Stabilizing ELAVL1 Protein. Molecular Biotechnology. 2023; 65: 1296–1305.

[4] An X, Xu G, Yang L, Wang Y, Li Y, McHepange UO, *et al*. Expression of hypoxia-inducible factor-1α, vascular endothelial growth factor and prolyl hydroxylase domain protein 2 in cutaneous squamous cell carcinoma and precursor lesions and their relationship with histological stages and clinical features. The Journal of Dermatology. 2014; 41: 76–83.

[5] Hu XL, Huang XT, Zhang JN, Liu J, Wen LJ, Xu X, *et al*. Long noncoding RNA MIR210HG is induced by hypoxia-inducible factor 1α and promotes cervical cancer progression. American Journal of Cancer Research. 2022; 12: 2783–2797.

[6] Jing X, Yang F, Shao C, Wei K, Xie M, Shen H, *et al*. Role of hypoxia in cancer therapy by regulating the tumor microenvironment. Molecular Cancer. 2019; 18: 157.

[7] Wicks EE, Semenza GL. Hypoxia-inducible factors: cancer progression and clinical translation. The Journal of Clinical Investigation. 2022; 132: e159839.

[8] Wolf KG, Crawford EB, Wartan NM, Schneiderman SK, Riehl VE, Dambaeva SV, *et al*. Ephrin-B2-expressing natural killer cells induce angiogenesis. JVS-Vascular Science. 2022; 3: 336–344.

[9] Yuan C, Wang P, Zhu S, Liu Z, Wang W, Geng T, *et al*. Overexpression of ephrinB2 in stem cells from apical papilla accelerates angiogenesis. Oral Diseases. 2019; 25: 848–859.

[10] Xie Y, Shi X, Sheng K, Han G, Li W, Zhao Q, *et al*. PI3K/Akt signaling transduction pathway, erythropoiesis and glycolysis in hypoxia (Review). Molecular Medicine Reports. 2019; 19: 783–791.

[11] Huang R, Zhang L, Jin J, Zhou Y, Zhang H, Lv C, *et al*. Bruceine D inhibits HIF-1α-mediated glucose metabolism in hepatocellular carcinoma by blocking ICAT/β-catenin interaction. Acta Pharmaceutica Sinica. B. 2021; 11: 3481–3492.

[12] Zhou Q, Yin Y, Yu M, Gao D, Sun J, Yang Z, *et al*. GTPBP4 promotes hepatocellular carcinoma progression and metastasis via the PKM2 dependent glucose metabolism. Redox Biology. 2022; 56: 102458.

[13] Bailleul J, Ruan Y, Abdulrahman L, Scott AJ, Yazal T, Sung D, *et al*. M2 isoform of pyruvate kinase rewires glucose metabolism during radiation therapy to promote an antioxidant response and glioblastoma radioresistance. Neuro-Oncology. 2023; 25: 1989–2000.

[14] Oh ST, Yang KJ, Bae JM, Park HJ, Yoo DS, Park YM. The differential expression of EPHB4 and ephrin B2 in cutaneous squamous cell carcinoma according to the grade of tumor differentiation: a clinicopathological study. International Journal of Dermatology. 2021; 60: 736–741.

[15] Liu W, Yu C, Li J, Fang J. The Roles of EphB2 in Cancer. Frontiers in Cell and Developmental Biology. 2022; 10: 788587.

[16] Al-Jamaei AAH, Subramanyam RV, Helder MN, Forouzanfar T, van der Meij EH, Al-Jamei S, *et al*. A narrative review of the role of Eph receptors in head and neck squamous cell carcinoma. Oral Diseases. 2023. (online ahead of print)

[17] Parlani M, Jorgez C, Friedl P. Plasticity of cancer invasion and energy metabolism. Trends in Cell Biology. 2023; 33: 388–402.

[18] Shang T, Li S, Zhang Y, Lu L, Cui L, Guo FF. Hypoxia promotes differentiation of adipose-derived stem cells into endothelial cells through demethylation of ephrinB2. Stem Cell Research & Therapy. 2019; 10: 133.

[19] Pan T, Sun S, Chen Y, Tian R, Chen E, Tan R, *et al*. Immune effects of PI3K/Akt/HIF-1α-regulated glycolysis in polymorphonuclear neutrophils during sepsis. Critical Care. 2022; 26: 29.

[20] Yang F, Zhang H, Mei Y, Wu M. Reciprocal regulation of HIF-1α and lincRNA-p21 modulates the Warburg effect. Molecular Cell. 2014; 53: 88–100.

[21] Wang JZ, Zhu W, Han J, Yang X, Zhou R, Lu HC, *et al*. The role of the HIF-1α/ALYREF/PKM2 axis in glycolysis and tumorigenesis of bladder cancer. Cancer Communications. 2021; 41: 560–575.

[22] Sesen J, Ghalali A, Driscoll J, Martinez T, Lupieri A, Zurakowski D, *et al*. Discovery and Characterization of Ephrin B2 and EphB4 Dysregulation and Novel Mutations in Cerebral Cavernous Malformations: In Vitro and Patient-Derived Evidence of Ephrin-Mediated Endothelial Cell Pathophysiology. Cellular and Molecular Neurobiology. 2023; 44: 12.

[23] Kischel A, Audouard C, Fawal MA, Davy A. Ephrin-B2 paces neuronal production in the developing neocortex. BMC Developmental Biology. 2020; 20: 12.

[24] Li T, Han J, Jia L, Hu X, Chen L, Wang Y. PKM2 coordinates glycolysis with mitochondrial fusion and oxidative phosphorylation. Protein & Cell. 2019; 10: 583–594.

[25] Zhang W, Zhang X, Huang S, Chen J, Ding P, Wang Q, *et al*. FOXM1D potentiates PKM2-mediated tumor glycolysis and angiogenesis. Molecular Oncology. 2021; 15: 1466–1485.

[26] Zhu S, Guo Y, Zhang X, Liu H, Yin M, Chen X, *et al*. Pyruvate kinase M2 (PKM2) in cancer and cancer therapeutics. Cancer Letters. 2021; 503: 240–248.

[27] Zahra K, Dey T, Ashish, Mishra SP, Pandey U. Pyruvate Kinase

M2 and Cancer: The Role of PKM2 in Promoting Tumorigenesis. Frontiers in Oncology. 2020; 10: 159.

[28] Chae HS, Hong ST. Overview of Cancer Metabolism and Signaling Transduction. International Journal of Molecular Sciences. 2022; 24: 12.

[29] Hu Z, Yu X, Ding R, Liu B, Gu C, Pan XW, *et al*. Glycolysis drives STING signaling to facilitate dendritic cell antitumor function. The Journal of Clinical Investigation. 2023; 133: e166031.

[30] Zheng YL, Li L, Jia YX, Zhang BZ, Li JC, Zhu YH, *et al*. LINC01554-Mediated Glucose Metabolism Reprogramming Suppresses Tumorigenicity in Hepatocellular Carcinoma via Downregulating PKM2 Expression and Inhibiting Akt/mTOR Signaling Pathway. Theranostics. 2019; 9: 796–810.

[31] Kierans SJ, Taylor CT. Regulation of glycolysis by the hypoxia-inducible factor (HIF): implications for cellular physiology. The Journal of Physiology. 2021; 599: 23–37.

[32] Hua Q, Mi B, Xu F, Wen J, Zhao L, Liu J, *et al*. Hypoxia-induced lncRNA-AC020978 promotes proliferation and glycolytic metabolism of non-small cell lung cancer by regulating PKM2/HIF-1α axis. Theranostics. 2020; 10: 4762–4778.

[33] Wang HJ, Hsieh YJ, Cheng WC, Lin CP, Lin YS, Yang SF, *et al*. JMJD5 regulates PKM2 nuclear translocation and reprograms HIF-1α-mediated glucose metabolism. Proceedings of the National Academy of Sciences of the United States of America. 2014; 111: 279–284.